REFERENCES

[1] A. A. Oliner, "Equivalent circuits for discontinuities in balanced strip transmission lines," *IRE Microwave Theory Tech.*, vol. MTT-3, pp. 134–143, Mar. 1956.

[2] H. M. Altschuler and A. A. Oliner, "Discontinuities in the centre conductor of symmetric strip transmission line," *IRE Trans. Microwave Theory Tech.*, vol. MTT-8, pp. 328–339, May 1960.

[3] I. J. Bahl and R. Garg, "A designer's guide to stripline circuits," *Microwaves*, vol. 17, no. 1, pp. 90–96, Jan. 1978.

[4] W. H. Leighton, Jr., and A. G. Milnes, "Junction reactance and dimensional tolerance effects on *X*-band, −3 dB directional couplers," *IEEE Trans. Microwave Theory Tech.*, vol. MTT-19, pp. 818–824, Oct. 1971.

[5] A. G. Franco and A. A. Oliner, "Symmetric strip transmission line tee junction," *IRE Trans. Microwave Theory Tech.*, vol. MTT-10, pp. 118–124, Mar. 1962.

[6] M. Dydyk, "Master the T-junction and sharpen your MIC designs," *Microwaves*, vol. 16, no. 5, pp. 184–186, May 1977.

[7] M. Cuhaci and G. J. P. Lo, "High frequency microstrip branch-line coupler design with T-junction discontinuity compensation," *Electron. Lett.*, vol. 17, no. 2, pp. 87–89, Jan. 22, 1981.

[8] R. Chadha and K. C. Gupta, "Compensation of discontinuities in planar transmission lines," *IEEE Trans. Microwave Theory Tech.*, vol. MTT-30, pp. 2151–2155, Dec. 1982.

[9] N. Marcuvitz, *Waveguide Handbook* (MIT Radiation Lab Series, vol. 10). New York: McGraw-Hill, 1949, pp. 336–339, 344–347, 363–368.

Power Increase of Pulsed Millimeter-Wave IMPATT Diodes

R. PIERZINA AND J. FREYER

Abstract—**The fabrication and encapsulation of single-drift pulsed IMPATT diodes for 73 GHz is described. The transforming properties of the parasitic inductance and capacitance demonstrate the strong influence of diode-mounting technique. The used reduced-height waveguide resonator is described theoretically, giving an indication of optimum matching between resonator and transformed diode impedance. The diodes deliver more than 10-W output power at 73 GHz with 5-percent efficiency, if they are matched to the resonator by proper parasitics.**

I. INTRODUCTION

At millimeter-wave frequencies, there is great interest in solid-state transmitters for radar, radiometry, or short-range communication systems. The high-power pulsed IMPATT diode has been proven to be the key element for these applications. Besides exact controllable semiconductor technology, packaging and circuit-mounting techniques are important factors for optimum performance. At microwave frequencies up to the *Ku*-band, semiconductor elements are either mounted in sealed metal–ceramic packages or are bonded directly into the microwave circuit [1], [2]. In contrast to these frequencies where the packaging technique normally will not limit the RF performance, the mounting parasitics at millimeter waves cause a transformation of the active diode impedance and usually limit output power and efficiency [1], [3]. Therefore, it is important to minimize the resistive parasitics associated with the diode chip and its mounting connections. The use of package parasitics for impedance matching [4], [5], however, shows that the often-stated demand of minimum parasitics [5], [6] does not lead automatically to the best RF performance results.

In this paper, design and fabrication of high-power pulsed IMPATT diodes for upper *V*-band frequencies are described. The output-power optimization is demonstrated by way of a single-drift diode because, in contrast to double-drift structures, only one active layer has to be adjusted. This, however, can easily be done by technological means [7]. The load impedance of the used resonator with reduced height is described in detail [8], representing the influence of the tuning elements. Since the diode impedance is transformed by the parasitic mounting capacitance and lead inductance, different encapsulation techniques of the diode are investigated. It is shown, that more than 10-W peak output power with 5-percent efficiency can be obtained if the diode impedance is well matched to the used resonator by proper parasitics.

Manuscript received May 31, 1984; revised May 15, 1985. This work was supported in part by Fraunhofer-Gesellschaft (FHG).

The authors are with the Technische Universität München, Lehrstuhl für Allgemeine Elektrotechnik und Angewandte Elektronik, Arcisstraße 21, D-8000 München 2, West Germany.

II. DEVICE FABRICATION

Initial material for the pulsed single-drift IMPATT diode is $n\text{-}n^+$ epitaxial silicon with a doping concentration of 6×10^{16} cm^{-3} of the n layer with thickness of 0.8 μm. The p-n junction is formed by a shallow boron diffusion resulting in a 0.55-μm-thick active layer designed for optimum frequencies in the upper *V*-band. The punch-through factor of the diodes is 1.8. The highly doped substrate is reduced by bubble etching to a thickness of only 1 or 2 μm in order to minimize losses due to the diode series resistance. This very thin substrate layer is also advantageous for short-pulse application of the diodes. In this case, the increase of the diode temperature during the current pulse is reduced as the heat flow is spread not only into the integrated heatsink but also into the bonding leads (25 μm) on top of the upside-down mounted diode. Single mesa-diodes with diameters between 100 and 200 μm for pulse operation in the *V*- and *W*-bands are obtained by standard photoresist technology. The individual diodes with integral Au-Ag-Au heatsinks are soldered on the gold-plated stud and quartz standoffs, as well as quartz and ceramic rings of various sizes, which are used for different mounting techniques. Hereby, the parasitic capacitance and inductance of the mounted devices can be varied in order to achieve optimum matching to the resonator.

III. MILLIMETER-WAVE CIRCUIT

At millimeter-wave frequencies, inductive-post or cap-type waveguide resonators are commonly used. The latter have been applied with great success in this laboratory for frequencies up to 140 GHz for CW IMPATT diodes mounted with very low parasitic capacitance and inductance [9], [10]. Single-drift pulsed IMPATT diodes mounted also with very low parasitics deliver about 5-W output power at *V*-band frequencies if they are operated in either a cap structure or an inductive-post resonator. Fig. 1 shows the cross section of an inductive-post resonator with reduced waveguide height. A detailed theoretical description of this resonator is given by Williamson [8] for low frequencies up to *Ku*-band and is adopted also for *V*-band frequencies. The diode is mounted on the bottom of the waveguide floor and the bias is provided through a choke with the inductive post. A sliding short behind the diode allows proper frequency and maximum output power tuning. Additionally, for impedance matching of the diode and the resonator, the post radius r_i and the length l_c of the coaxial section can be varied. The waveguide height is reduced and a taper connects the resonator with the WR-15 waveguide measuring system. Taking into account perfect matching at both waveguide arms and, for example $l_c = 0$, the real and imaginary parts of the circuit impedance Z_c presented to the diode are plotted in Fig. 2 as functions of the reduced waveguide height b.

0018-9480/85/1100-1228$01.00 ©1985 IEEE

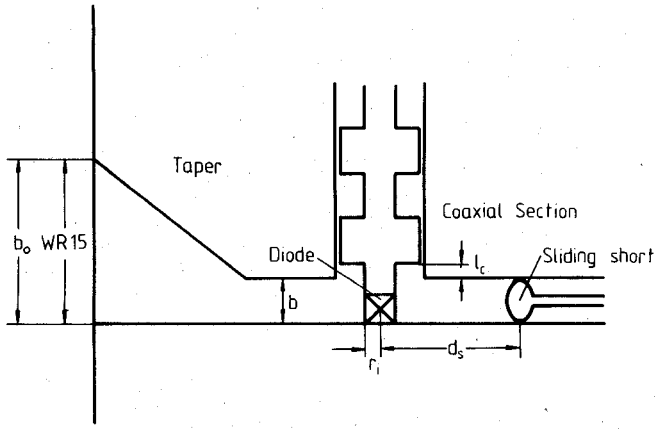

Fig. 1. Cross section of an inductive-post resonator with reduced waveguide height.

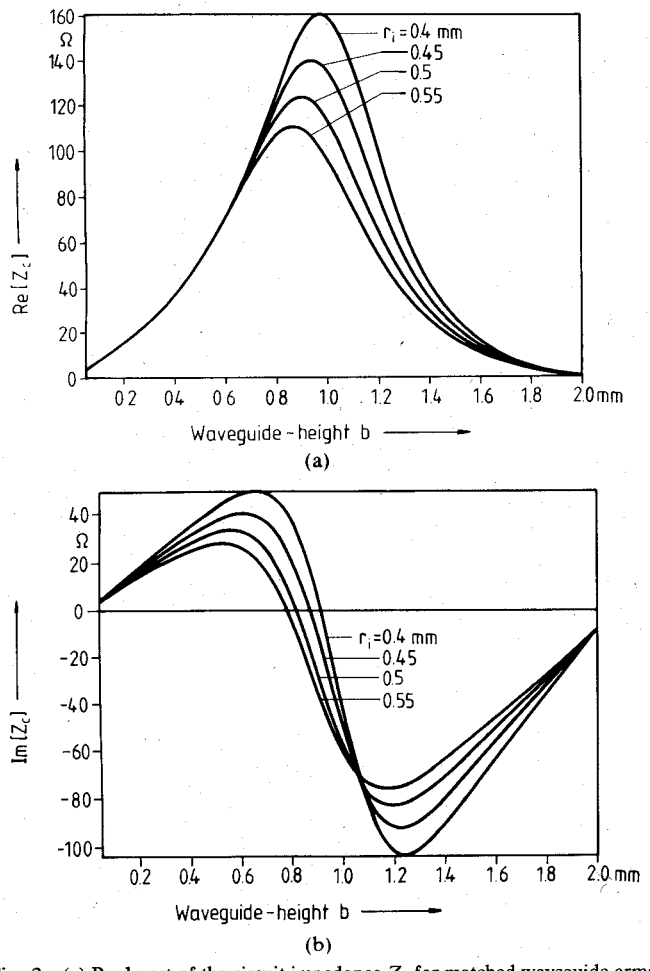

Fig. 2 (a) Real part of the circuit impedance Z_c for matched waveguide arms, $f = 73$ GHz. (b) Imaginary part of the circuit impedance Z_c for matched waveguide arms, $f = 73$ GHz.

Curves for various values of the radius r_i of the inductive post are shown. As can be seen, two characteristic ranges with different impedance levels can be determined. Relatively small values for the real and imaginary parts of Z_c are obtained if the waveguide height is either strongly reduced or nearly unreduced. For medium reduction, a resonance occurs, i.e., $\mathrm{Re}\{Z_c\}$ (Fig. 2(a)) becomes relatively large and $\mathrm{Im}\{Z_c\}$ (Fig. 2(b)) changes between inductive and capacitive reactance. Except at this resonance, the diameter of the inductive post has little influence on the impedance. The strongly reduced waveguide resonator represents the most

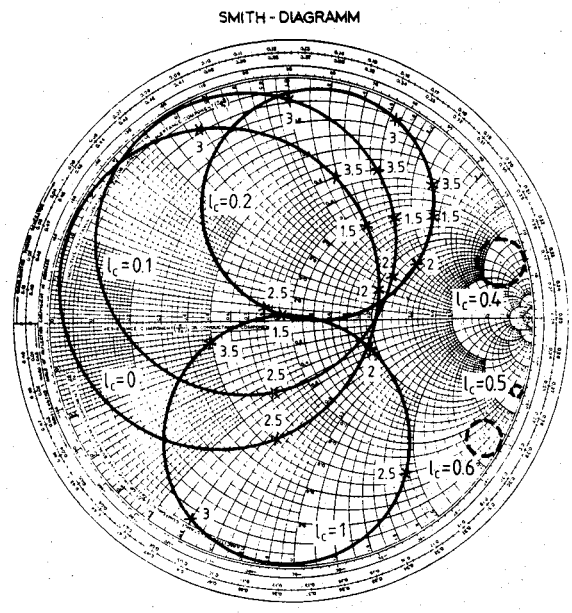

Fig. 3. Circuit impedance Z_c as a function of the coaxial section length l_c and distance d_s between sliding short and diode. (The waveguide wavelength is 5 mm; l_c and d_s in mm; $Z_o = 50\ \Omega$, $f = 73$ GHz.)

commonly used one for pulsed and CW IMPATT diodes at millimeter-wave frequencies and is also investigated in this laboratory in detail.

The description of the resonator impedance becomes relatively difficult to survey if the location of the sliding short and the length of the coaxial section l_c are also varied. The Smith Chart in Fig. 3 demonstrates the tuning behavior of the resonator as shown in Fig. 1 for a reduced waveguide height ($b = 0.5$ mm) and an inductive post of 1-mm diameter. The circles show the typical behavior of periodic tuning by the sliding short for different values of l_c (from 0 to 1 mm) as a parameter. The numbers at the circles denote the distance d_s in millimeters of the sliding short from the center of the diode. It can be seen that theoretically a large area in the Smith Chart can be covered by changing l_c and d_s. For certain l_c values, Z_c shows a distinct resonance behavior, as can be seen by the dotted circles. In this resonance vicinity, small changes in l_c and d_s, respectively, cause relatively large changes in Z_c. In practice, proper diode tuning, therefore, becomes impossible. In Fig. 5, it will be shown that the transformed diode impedance Z_T—off the resonance—is inductive or capacitive with a relatively low real part. Thus, diode/resonator matching can be achieved in the following two cases.

1) For a length of the coaxial section of, for example, 1 mm, a capacitive reactance with low real part can be realized if the sliding-short has a distance between 2.5 and 3 mm. In this case, however, tuning is relatively critical, since small deviations in the sliding-short produce large changes in the imaginary part.

2) The demand of a low real part can also be fulfilled by low values of l_c (between 0 and 0.2 mm). Here an inductive behavior follows, and the distance between diode and short may vary between 3 and 3.5 mm. In contrast to the first case, tuning is less critical, because a small deviation in the sliding-short distance leads to only small deviations in the resonator impedance.

IV. Diode Impedance Transformation

Normally the small-signal characteristic of the diode impedance is used for a first-order estimation. However, since pulsed IMPATT diodes are operated at very high current densities (5×10^4 A/cm^2 at V-band) in order to deliver maximum output

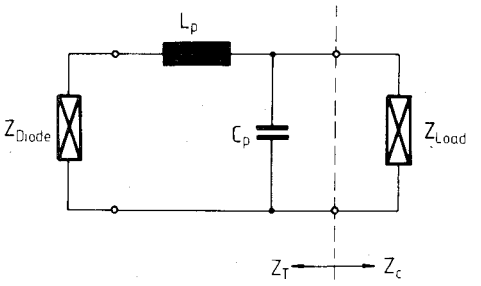

Fig. 4. Matching network.

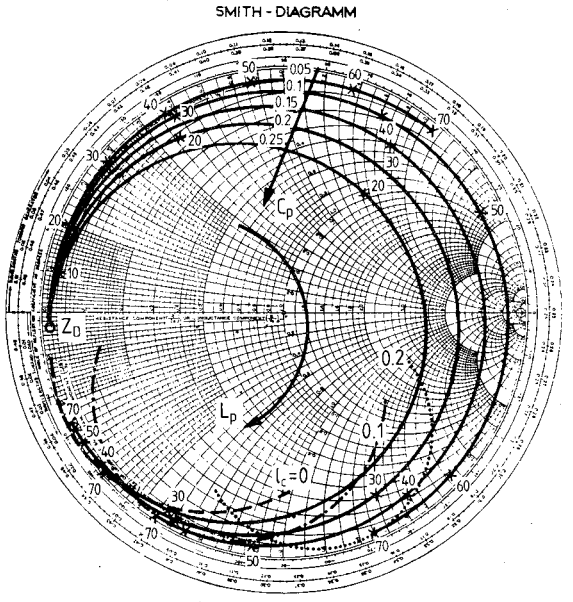

Fig. 5. Contours of the transformed diode impedance Z_T as a function of L_p/pH and C_p/pF. The dotted lines represent the conjugate complex of Z_c (see Fig. 3) corresponding to $l_c = 0, 0.1, 0.2$ mm; $Z_o = 50\ \Omega$; $f = 73$ GHz.

power, and since the oscillation frequency and the negative resistance are strongly dependent on the current density, small-signal impedance differs considerably from the actual large-signal impedance. Therefore, in this case, the large-signal impedance Z_D is taken as a basis, and diode impedance calculations are carried out by means of the following description [11]:

$$Z_D = \frac{1}{\omega C_d} \cdot \frac{(1-\cos\theta)/\theta}{1-(\omega/\omega_a(u))^2} - j\left[\frac{1}{\omega C_d}\cdot\left(1-\frac{\sin\theta/\theta}{1-(\omega/\omega_a(u))^2}\right)+\frac{1}{\omega C_a}\cdot\frac{1}{1-(\omega_a(u)/\omega)^2}\right].$$

Here, ω is the angular frequency and $\omega_a(u)$ the RF voltage-dependent avalanche frequency given by

$$\omega_a^2(u) = \frac{2\alpha' v_s J_0}{\epsilon}\cdot\frac{2I_1(u)}{uI_0(u)}$$

and

$$u = \frac{2\alpha' v_s}{\omega}\hat{E}_a$$

where α' is the derivative of the ionization rate with respect to the electric field, v_s is the carrier saturation drift velocity, J_0 is the dc current density, θ is the transit angle, $I_0(u)$ and $I_1(u)$ denote modified Bessel functions, and C_a and C_d are the avalanche and drift region capacitance, respectively. $\hat{E}_a$ corresponds to the maximum amplitude of the RF field at the avalanche region and is assumed to be 0.4 times the dc breakdown field [12]. Of course the diode impedance depends on the current density. For maximum output power, however, $J_0 = 50$ kA/cm^2 was taken as a basis [12], [13]. From this evaluation, the real and imaginary parts of the diode impedance per unit area of about $-8\cdot10^{-5}\ \Omega$ cm^2 and $-3\cdot10^{-4}\ \Omega$ cm^2, respectively, can be assumed. For a typical V-band pulsed IMPATT diode with 165-μm diameter, a value for the negative resistance of about 0.4 Ω and for the imaginary part of $-1.4\ \Omega$ follows at 73 GHz.

These small values for the real and imaginary parts must be matched by means of the mounting parasitic capacitance C_p and inductance L_p to the resonator impedance Z_c. As maximum output power is required in the range from 70–75 GHz, a narrow-band characteristic of the diode behavior must be tolerated. A simple equivalent circuit of the matching network is given in Fig. 4 [4], [14] where C_p represents the quartz ring or stand-off capacitance and L_p the bonding lead inductance. The Smith Chart in Fig. 5 shows the diode impedance Z_D and the loci of the transformed impedance Z_T as a function of the parasitic inductance with parasitic capacitance as parameter. Capacitance and inductance pass through typical values which can be obtained by different mounting techniques.

For stable oscillations, the sum of the transformed diode and the resonator impedance must be zero, i.e., for an inductive resonator the transformed diode impedance must be capacitive and vice versa. As can be seen in Fig. 5, low values of C_p and L_p cause a transformation of the capacitive diode impedance to inductive behavior with a low real part. The corresponding resonator impedance therefore has to be capacitive with also a low real part (see Section III). From the point of view of reproducibility, however, it is relatively difficult to realize technologically very low L_p and C_p concurrently. Besides the critical tuning of the resonator (see Section III), small deviations in L_p and C_p affect the optimum frequency and maximum output power. For relatively larger values of L_p and C_p, the diode impedance can be transformed to capacitive behavior with also low negative resistance. In this case, a resonator with inductive behavior is needed which can be realized for example by low values of l_c (see Section III). Stable oscillations are then given by the intersection points of the diode and the dotted resonator contours shown in Fig. 5. The latter represent parts of the complex conjugate of the impedance Z_c shown in Fig. 3 corresponding to $l_c = 0$, 0.1, and 0.2 mm. It can be seen that for these l_c values, resonator tuning with the backshort can be obtained for the transformed diode impedance with mounting parasitics which can vary in a relatively large range (L_p: 25–70 pH; C_p: 0.1–0.3 pF).

V. Results

The investigations of the diodes are carried out in a reduced-height waveguide resonator ($b = 0.5$ mm) with a length of the coaxial section of $l_c = 0.15$ mm, which allows optimum matching of a low real part with capacitive reactance. The diodes are driven with 50-ns pulses and a duty cycle of 1:200 up to maximum current densities of 50 kA/cm^2. Maximum output power was obtained at 73 GHz. The experimental results of the investigated single-drift IMPATT diodes are summarized in Table I.

All diodes originate from the same batch, however, with different areas and encapsulation techniques. The diodes in column 1 to 4 are mounted in commercially available packages with ceramic rings. The top of the diode is connected with the metallized ring by two cross-wise bonded gold leads (25 μm$\times$110 μm). The investigated diodes have areas from $1.4\cdot10^{-4}$ to $2.7\cdot10^{-4}$ cm^2. As can be seen, output power increases from 6 W for diode #1 to 8.9 W for diode #3 because of increasing diode area. For still larger areas (diode #4), the output power decreases since the

TABLE I

Diode #	1	2	3	4	5	6	7
	ceramic	ceramic	ceramic	ceramic	quartz	quartz	quartz
A/cm^2 x 10^{-4}	1.4	1.9	2.4	2.7	2.4	2.4	2.4
C_p* /pF	0.22	0.22	0.22	0.22	0.08	0.28	0.2
L_p** /pH	30	30	30	30	30	20	45
P/W	6	7.5	8.9	6.5	3.8	8.1	10.2

*C_P is measured by a Boonton RF admittance bridge.
**L_p is evaluated from inductance values published by Kramer [1] and Chang and Ebert [13].

very low negative diode resistance favors diode internal and circuit losses.

If, instead of the ceramic ring (diodes #1–4), a quartz ring with nearly the same dimension (diode #5) is used, the capacitance C_p reduces from 0.22 pF to 0.08 pF and the inductance remains constant. The maximum output power of this type of encapsulated diode, however, is only 3.8 W, though the diode is the same as diode #3 and a low-loss quartz ring is applied. In the case of the used resonator, this behavior can be explained with the aid of Figs. 3 and 5. The resonator is optimized to match a low negative real part with capacitive reactance (see Fig. 3; $l_c = 0.15$ mm). The ceramic ring in addition with the cross-wise bonded gold stripes of diodes #1–4 leads to a transformation with this capacitance character (see Fig. 5, lower half of the Smith Chart), and good matching of the transformed diode and the resonator is possible. The quartz ring, however, with the same bonding lead inductance causes a transformation with inductive character where an optimum matching of the resonator cannot be obtained and only 3.8-W output power can be achieved. Referring to the data of diode #6, a larger value of the capacitance C_p (0.28 pF) in addition with a relatively low inductance L_p (20 pH) leads to a transformation with again capacitive behavior and correspondingly higher output power of 8.1 W can be obtained. A further increase in output power for the same diodes is achievable if the value of the inductance L_p is further increased (to 45 pH for diode #7), and in this case a maximum output power of more than 10 W at 5-percent efficiency was obtained. These results reflect that, depending on the resonator properties, even relatively large parasitics allow an optimum matching if the resonator and the diode transforming network are well designed.

VI. Conclusion

The fabrication of pulsed single-drift IMPATT diodes for millimeter-wave frequencies with different mounting techniques has been described. An inductive-post resonator with reduced waveguide height enables an efficient matching so that more than 10-W peak output power at 5-percent efficiency can be achieved, demonstrating that the single-drift diode can compete with double-drift devices at *V*-band frequencies. The knowledge of the resonator and diode impedance allows a prediction of the needed parasitic reactances which transform the diode impedance for optimum matching. In contrast to the often-stated demand of minimum parasitics, the results show that a relatively large and not a minimum value for the inductance of the connecting lead delivers maximum output power.

Acknowledgment

The authors are very indebted to Dr. A.G. Williamson for sending some of his "School of Engineering Reports." They wish to acknowledge Prof. W. Harth for helpful discussions.

References

[1] N. B. Kramer, "Millimeter-wave semiconductor devices," *IEEE Trans. Microwave Theory Tech.*, vol. MTT-24, pp. 685–693, 1976.
[2] R. J. Wagner, W. W. Gray, and P. V. Cooper, "*X*-band IMPATT microstrip power sources," *IEEE J. Solid-State Circuits*, vol. SC-3, pp. 221–225, 1968.
[3] K. P Weller, R. S. Ying, and D. K. Lee, "Pumps and local oscillators," Air Force Avionics Lab., Tech. Rep. AFAL-TR-75-177, Sept. 1975.
[4] H. J. Kuno and D. L. English, "Nonlinear and large-signal characteristics of millimeter-wave IMPATT amplifiers," *IEEE Trans. Microwave Theory Tech.*, vol. MTT-21, pp. 703–706, 1973.
[5] T. A. Midford and R. L. Bernick, "Millimeter-wave CW IMPATT diodes and oscillators," *IEEE Trans. Microwave Theory Tech.*, vol. MTT-27, pp. 483–492, 1979.
[6] A. R. Kerr, "Low-noise room-temperature and cryogenic mixers for 80–120 GHz," *IEEE Trans. Microwave Theory Tech.*, vol. MTT-23, pp. 781–787, Oct. 1975.
[7] R. Pierzina, to be published.
[8] A. G. Williamson, "Analysis and modeling of two-gap coaxial line rectangular waveguide junctions," *IEEE Trans. Microwave Theory Tech.*, vol MTT-31, pp. 295–302, 1980.
[9] D. Leistner, "Herstellung und Untersuchung von Lawinenlaufzeitdioden und Oszillatoren für *V*- and *W*-Band-Frequenzen," Diss. Techn. Univ. München, 1983.
[10] J. Wenger, "140 GHz 70 mW CW output power with n-type silicon single-drift IMPATT diodes," *Electron. Lett*, vol. 19, pp. 908–909, 1983.
[11] H. G. Unger and W Harth, *Hochfrequenz-Halbleiterelektronik*. Stuttgart: S. Hirzel Verlag, 1972.
[12] W. Harth and M. Claassen, *Aktive Mikrowellendioden*. Berlin: Springer-Verlag, 1981.
[13] S. O'Hara and J. R. Grierson, "A study of the power handling ability of gallium arsenide and silicon, single and double drift impatt diodes," *Solid-State Electron*, vol. 17, pp. 137–153, 1974.
[14] K. Chang and R. L. Ebert, "*W*-band power combiner design," *IEEE Trans. Microwave Theory Tech.*, vol. MTT-28, pp. 295–305, 1980.

X-Band Low-Noise GaAs Monolithic Frequency Converter

K. HONJO, Y. HOSONO, AND T. SUGIURA

***Abstract*—An *X*-band, low-noise GaAs monolithic frequency converter has been developed. Multicircuit functions, such as amplification, filtering, and mixing, were integrated on to a single GaAs frequency converter chip. The frequency converter consists of an *X*-band three-stage low-noise amplifier, an image rejection filter, an *X*-band dual-gate FET mixer, and an IF-band buffer amplifier. To minimize circuit size without degrading performances, an *RC*-coupled buffer amplifier was connected directly after a dual-gate FET mixer IF port, and one-section parallel and series microstrip lines were adopted for the amplifier. One-half-micron (1/2 μm) single-gate FET's and a one-micron (1 μm) dual-gate FET, which have an ion-implanted closely-spaced electrode structure, were used. Either via hole grounds or bonding wire grounds are selectable for the frequency converter. Chip size is 3.4×1.5 mm. The frequency converter provides less than 3-dB noise figure and more than 34-dB conversion gain.**

Manuscript received December 18, 1984; revised July 2, 1985.

K. Honjo is with the Microelectronics Research Laboratories, NEC Corporation, 1-1 Miyazaki, 4-chome, Miyamae-ku, Kawasaki, Kanagawa 213, Japan.
Y. Hosono is with the NEC Corporation, Second LSI Division, Kawasaki, Kanagawa 213, Japan.
T. Sugiura is with the NEC corporation, Space Laser Communication Division, Kawasaki, Kanagawa, Japan.

0018-9480/85/1100-1231$01.00 ©1985 IEEE